

NASA Technical Memorandum 106380  
ICOMP-93-42  
AIAA-93-3368

11-34  
143176  
13P

# On Solving the Compressible Navier-Stokes Equations for Unsteady Flows at Very Low Mach Numbers

R.H. Pletcher  
*Institute for Computational Mechanics in Propulsion  
Lewis Research Center  
Cleveland, Ohio*

*and Iowa State University  
Ames, Iowa*

and

K.-H. Chen  
*Ohio Aerospace Institute  
Brook Park, Ohio*

*and University of Toledo  
Toledo, Ohio*

Prepared for the  
24th Fluid Dynamics Conference  
sponsored by the American Institute of Aeronautics and Astronautics  
Orlando, Florida, July 6-9, 1993

**NASA**

N94-17128

Unclas

G3/34 0193176

(NASA-TM-106380) ON SOLVING THE  
COMPRESSIBLE NAVIER-STOKES  
EQUATIONS FOR UNSTEADY FLOWS AT  
VERY LOW MACH NUMBERS (NASA) 13 P





# ON SOLVING THE COMPRESSIBLE NAVIER-STOKES EQUATIONS FOR UNSTEADY FLOWS AT VERY LOW MACH NUMBERS

R.H. Fletcher

Institute for Computational Mechanics in Propulsion  
Lewis Research Center  
Cleveland, Ohio 44135

and Iowa State University  
Ames, Iowa

and

K.-H. Chen

Ohio Aerospace Institute  
22800 Cedar Point Road  
Brook Park, Ohio 44142

## ABSTRACT

The properties of a preconditioned, coupled, strongly implicit finite-difference scheme for solving the compressible Navier-Stokes equations in primitive variables are investigated for two unsteady flows at low speeds, namely the impulsively started driven cavity and the startup of pipe flow. For the shear-driven cavity flow, the computational effort was observed to be nearly independent of Mach number, especially at the low end of the range considered. This Mach number independence was also observed for steady pipe flow calculations; however, rather different conclusions were drawn for the unsteady calculations. In the pressure-driven pipe startup problem, the compressibility of the fluid began to significantly influence the physics of the flow development at quite low Mach numbers. The present scheme was observed to produce the expected characteristics of completely incompressible flow when the Mach number was set at very low values. Good agreement with incompressible results available in the literature was observed.

## INTRODUCTION

Over the past few years a more complete understanding of the behavior of numerical algorithms for solving the time-dependent, compressible Navier-Stokes equations at low Mach numbers has evolved. Until this understanding developed, most algorithms designed for compressible flows were observed to become very inefficient, or inaccurate, or both at low Mach numbers. This is unnecessary because it is well known that the physics itself is no more complex just because the Mach number is low. That is, for most flows, no important changes would be observed if the Mach number were reduced from, say, 0.2 to 0.01, if all other dimensionless parameters of the flow remained the same. The difficulty must be due to an inappropriate structure of the algorithm. This problem and proposed remedies have been addressed by several investigators including Turkel<sup>1,2</sup>, Feng and Merkle<sup>3</sup>, Peyret and Viviani<sup>4</sup>, and Choi and Merkle<sup>5</sup>.

Previous investigators have adopted different points of view but have generally agreed that the hyperbolic time-dependent Navier-Stokes system becomes "stiff" at low Mach numbers because of greatly different signal speeds (convective and acoustic) which result in large differences in the magnitudes of the eigenvalues of the system. Explicit schemes especially

are restricted to using very small time steps as dictated by stability based on acoustic speeds. Fluid particles, on the other hand, may require several of these small time steps to traverse a computational cell. As pointed out by Choi and Merkle<sup>5</sup> difficulties at low Mach numbers with implicit factored schemes may be due in large part to factorization errors unless the time step is maintained quite small. The alterations made to the numerical formulation to overcome the stiffness problems of the hyperbolic system has become known as "preconditioning" which will be discussed in physical terms in a section to follow. Despite this name which may be adequately descriptive from some points of view, the preconditioned system is merely one with a "modified" time term. This can be made to appear in the equations as a new matrix multiplying the time term in the vector form of the system of equations. To solve *steady* problems, the preconditioning can be accomplished by altering the time derivative term in the equations. To solve *unsteady* problems, the physical time term can be left intact and an additional "pseudo-time" term of a particular form added to the equations. These altered or added time terms change the nature of the hyperbolic problem which is being advanced in a "new" or "pseudo" time variable. Because all the altered time terms vanish at convergence (to steady state or at each physical time step), no approximation is being injected into the governing equations. Essentially, in the low Mach number limit, the preconditioning enables the numerical model to smoothly bridge the gap between a fully compressible formulation and one that can, for isothermal flows, be viewed as a pseudo-compressible formulation<sup>6</sup> of the incompressible equations.

Low speed flows can, of course, be computed by using a completely incompressible formulation. One of the objectives of the present paper is to suggest that a properly formulated compressible formulation can be applied to flows that have been traditionally considered incompressible with essentially no penalty in accuracy or computational efficiency. It would seem that the computational barrier between the two flow regimes has been broken. The compressible flow formulation may be advantageous for low speed flows in which properties, including density, may vary significantly such as would occur in flows with heat transfer or chemical reactions.

A second objective of the present paper is to examine the properties of a particular preconditioned formulation for some unsteady flows, namely the impulsively started driven cavity and the startup of pipe flow. Most of the early work on preconditioning concentrated on formulations for steady flows.

Time-accurate preconditioning has been introduced relatively recently and the properties of such schemes for the Navier-Stokes equations have not been studied extensively over a range of flow configurations and Mach numbers. Whereas the merits of time-accurate formulations of Mach number preconditioned systems may have been demonstrated for the very low speed limit<sup>7</sup>, their accuracy and convergence have not been demonstrated over a very wide range of problems and Mach numbers. An additional minor goal of this paper is to supplement the discussions on preconditioning available in the literature with some physically based arguments and observations.

In this study, the coupled strongly implicit procedure for solving the Navier-Stokes equations in primitive variables described in Ref. [8] was used as a starting point. In the sections to follow, the modifications required to achieve convergence properties that are independent of Mach number at low speeds are first discussed in a one-dimensional context, then their implementation into the full two-dimensional Navier-Stokes equations is presented. Steady and unsteady results with and without preconditioning will be presented for the driven cavity problem. Results for the startup of pipe flow under a fixed total pressure will also be presented. The transient pipe flow problem was selected because it is one of the few physically attainable transient flows for which results are available for comparison.

## ANALYSIS

### Low Mach Number Limit

It is well established that the incompressible form (including variable property versions) of the Navier-Stokes equations can be solved numerically in a straightforward manner. To reveal the source of the numerical difficulty that arises in solving the compressible form of the Navier-Stokes equations at low Mach numbers, we first examine the compressible Navier-Stokes equations in a form that should reduce to the incompressible but variable property form of the Navier-Stokes equations as the Mach number approaches zero. The density and other fluid properties may vary with temperature, but we anticipate that the density will become independent of pressure as the Mach number approaches zero.

The key issues can be outlined sufficiently by using the one-dimensional Navier-Stokes equations. Nondimensional variables are defined as

$$\begin{aligned} t &= \frac{\tilde{t}}{L_{ref}/u_{ref}}, \quad x = \frac{\tilde{x}}{L_{ref}}, \quad u = \frac{\tilde{u}}{u_{ref}}, \quad \rho = \frac{\tilde{\rho}}{\rho_{ref}}, \\ p &= \frac{\tilde{p}}{(\rho_{ref} u_{ref}^2)}, \quad T = \frac{\tilde{T}}{T_{ref}}, \quad \mu = \frac{\tilde{\mu}}{\mu_{ref}}, \\ R &= \frac{\tilde{R}}{(u_{ref}^2/T_{ref})} = \frac{1}{\gamma M^2}, \\ C_p &= \frac{\tilde{C}_p}{(u_{ref}^2/T_{ref})} = \frac{1}{(\gamma - 1)M^2} \end{aligned}$$

where the variables with the tilde are the dimensional variables, and the Mach number,  $M$ , is based on reference quantities and the gas constant,  $M = u_{ref}/(\gamma \tilde{R} T_{ref})^{1/2}$ . In order to recover the incompressible form of the equations in the most

direct manner, primitive variables of  $u$ ,  $p$ , and  $T$  will be used in the one-dimensional compressible formulation. There are no known disadvantages to the use of the primitive variables, particularly if the conservation law form of the equations is maintained. Substituting for density by using the ideal gas equation of state and utilizing primitive variables,  $p$ ,  $u$ , and  $T$ , the conservation equations for mass, momentum and energy can be written

$$\frac{\partial Q(\bar{q})}{\partial t} + \frac{\partial E(\bar{q})}{\partial x} - \frac{\partial E_v(\bar{q})}{\partial x} = 0 \quad (1)$$

where

$$\begin{aligned} \bar{q} &= \begin{pmatrix} p \\ u \\ T \end{pmatrix} \quad Q = \begin{pmatrix} \frac{p}{RT} \\ \frac{pu}{RT} \\ \frac{p}{\gamma R} + M^2 \frac{(\gamma-1)}{2} \frac{pu^2}{RT} \end{pmatrix} \\ E &= \begin{pmatrix} \frac{pu}{RT} \\ \frac{pu^2}{RT} + p \\ \frac{pu}{R} + M^2 \frac{(\gamma-1)}{2} \frac{pu^3}{RT} \end{pmatrix} \\ E_v &= \begin{pmatrix} 0 \\ \frac{4\mu}{3Re} \frac{\partial u}{\partial x} \\ \frac{4(\gamma-1)M^2\mu}{3Re} \frac{\partial u}{\partial x} + \frac{\mu}{RePr} \frac{\partial T}{\partial x} \end{pmatrix} \end{aligned}$$

The Reynolds and Prandtl numbers are defined as  $Re = \rho_{ref} u_{ref} L_{ref} / \mu_{ref}$ ,  $Pr = \tilde{C}_p \tilde{\mu} / \tilde{k}$ . The Prandtl number of the fluid is assumed to be constant. Now the consequences of the reference Mach number approaching zero will be considered. Note that  $p/RT = \tilde{\rho}/\rho_{ref}$  and  $R = 1/(\gamma M^2)$ . We observe that the combination  $p/RT$  approaches a perfectly acceptable finite limit as  $M$  goes to zero. Note that  $E$  and  $E_v$  will reduce to the traditional form of the incompressible Navier-Stokes equations as the Mach number approaches zero. The numerical solution will require linearization which can be accomplished by introducing Jacobian matrices which can be updated iteratively at each time step. This linearization is equivalent to solving

$$[A_t] \frac{\partial \bar{q}}{\partial t} + [A_x] \frac{\partial \bar{q}}{\partial x} = \frac{\partial E_v}{\partial x} \quad (2)$$

where the Jacobian matrices for the mass and momentum fluxes are given by

$$[A_t] = \begin{bmatrix} \frac{\gamma M^2}{T} & 0 & -\frac{p}{RT^2} \\ \frac{\gamma M^2 u}{T} & \frac{p}{RT} & -\frac{pu}{RT^2} \\ M^2 + \gamma M^4 \frac{u^2(\gamma-1)}{2T} & \gamma M^4 \frac{u(\gamma-1)}{T} & -\gamma M^4 \frac{pu^2(\gamma-1)}{2T^2} \end{bmatrix}$$

and

$$[A_x] = \begin{bmatrix} \frac{\gamma M^2 u}{T} & \frac{p}{RT} & -\frac{pu}{RT^2} \\ \frac{\gamma M^2 u^2}{T} + 1 & \frac{2pu}{RT} & -\frac{pu^2}{RT^2} \\ -\gamma M^4 \frac{u^2(\gamma-1)}{2T} & \frac{2}{T} + \gamma M^4 \frac{u^2(\gamma-1)}{2T} & -\gamma M^4 \frac{pu^2(\gamma-1)}{2T^2} \end{bmatrix}$$

The linearization details for the viscous terms are being omitted since these terms do not influence the low Mach number issues under consideration here. In the above,  $R$  has

been replaced by  $1/(\gamma M^2)$  in those terms that will vanish as  $M$  goes to zero. Notice that the variable property form of the equations usually applied for low speed flow of an ideal gas are recovered as  $M$  goes to zero. The mathematical nature of the time marching problem can be established by writing the system as

$$\frac{\partial \vec{q}}{\partial t} + [A_t]^{-1} [A_x] \frac{\partial \vec{q}}{\partial x} = [A_t]^{-1} \frac{\partial E_v}{\partial x} \quad (3)$$

and considering the eigenvalues of  $[A_t]^{-1} [A_x]$ . The problem can be solved by a marching method if the eigenvalues are real. As  $M$  becomes small,  $[A_t]$  becomes ill-conditioned. That is, the determinant of  $[A_t]$  becomes small (in fact, in the limit the first column and third row of  $[A_t]$  vanish) and errors are expected to arise in computing its inverse. In the limit as  $M$  goes to 0, the inverse of  $[A_t]$  does not exist and the system is singular.

It is well-known that the eigenvalues of the matrix product  $[A_t]^{-1} [A_x]$  also provide an indication of the properties of the system. As the Mach number is decreased in the subsonic regime, the eigenvalues of the matrix product  $[A_t]^{-1} [A_x]$  begin to differ more and more in magnitude (see for example, Turkel<sup>1</sup>). As pointed out by previous investigators<sup>2,3</sup> the condition and degree of "stiffness" can be related to the relative magnitudes of the eigenvalues. When the eigenvalues differ greatly in magnitude, convergence to a steady state solution is usually slow, or for time-dependent solutions, the allowable time step becomes very small. This occurs because greatly varying signal speeds appear in the equations and the traditional solution schemes attempt to honor all of them, creating a "stiff" system. Since the Mach number has almost no influence on the physical characteristics of the flow at very low values of  $M$  (it effectively "cancels out" of the physics), it must be possible to devise a solution scheme in which the Mach number also "cancels out" over the range in which it is an unimportant physical parameter.

It can be observed from  $[A_t]$  that as the Mach number approaches zero, the pressure is eliminated as an unknown in the time derivative. This indicates that the solution to the incompressible equations carry no direct pressure history. Although the pressure field may not change much during a time step, in principle, the new pressure should depend solely on the new velocity field. Because the acoustic speed is effectively infinite in the incompressible limit, the pressure at a point may be influenced by the velocity field throughout the solution domain. A time-accurate compressible flow solution scheme must then provide a mechanism to permit the pressure field to be influenced in an elliptic fashion at each time step.

### Overcoming the Problem at Low Mach Numbers

To overcome the awkward (singular) mathematical situation that arises at low Mach numbers with the unsteady form of the coupled compressible equations and obtain a well-conditioned system, an appropriately formulated pseudo-time term can be added to the equations which vanishes at convergence at each physical time. Although the pseudo-time term can take many different forms and still be effective, simply adding a term of the same form as for the physical time term but with the Mach number removed from the terms causing the fatal ill-conditioning (the first column of the  $[A_t]$  matrix) is sufficient. The equations then become

$$[A_p] \frac{\partial \vec{q}}{\partial \tau} + [A_t] \frac{\partial \vec{q}}{\partial t} + [A_x] \frac{\partial \vec{q}}{\partial x} = \frac{\partial E_v}{\partial x} \quad (4)$$

where  $\tau$  is a pseudo-time and the conditioning matrix,  $[A_p]$  is given by

$$[A_p] = \begin{bmatrix} \frac{1}{\gamma} & 0 & -\frac{p}{RT^2} \\ \frac{1}{\gamma} + M^2 u^2 \frac{(\gamma-1)}{2T} & \frac{p}{RT} & -\frac{pu}{RT^2} \\ \frac{1}{\gamma} + M^2 v^2 \frac{(\gamma-1)}{2T} & \gamma M^4 p \frac{(\gamma-1)u}{T} & -\gamma M^4 p u^2 \frac{(\gamma-1)}{2T^2} \end{bmatrix}$$

Notice that  $[A_p]$  is formed from  $[A_t]$  by simply dividing the first column of  $[A_t]$  by  $\gamma M^2$  (equivalent to multiplying by the nondimensional gas constant  $R$ ). Presumably, dividing by only  $M^2$  would have the same effect.

The hyperbolic system can be solved by advancing in pseudo-time until no changes occur at each physical time step. At that point, the time-accurate equations are satisfied. Obviously, this involves "subiterations", but that is consistent with the observation that for a completely incompressible flow, the pressure field must be established at each physical time step with no direct dependence on a previous pressure field as was mentioned above. The hyperbolic system being solved is in  $\tau$  and  $x$ . It is similar to marching in pseudo-time to a "steady" solution at each physical time step. The addition of the pseudo-time term changes the eigenvalues of the hyperbolic system so that they are clustered closer together in magnitude, effectively at speeds closer to the convective speed. Eigenvalues for this system have been studied by Jorgenson<sup>9</sup> and found to be similar to those reported by Withington et al.<sup>10</sup> As the Mach number goes to zero, the ratio of the largest to smallest eigenvalues approaches 2.27 for air with  $\gamma=1.4$ .

The second and minor source of difficulty with the coupled compressible formulation at low Mach numbers is related to the differences in the relative magnitudes of the nondimensional dependent variables. The magnitudes of the velocity and temperature remain of order one but the nondimensional pressure tends to increase without limit as the Mach number decreases. This permits round-off errors to become significant in the pressure gradient terms. Again, this is not a problem of physical origin. The present study indicated that no difficulties will usually be observed until the Mach number decreases to about  $10^{-5}$  or  $10^{-6}$  if double precision arithmetic is used. To completely eliminate the problem, a "gauge" or relative pressure<sup>3</sup> can be introduced so that differences in pressure (originating from pressure derivatives) become differences in the gauge pressure which can then be smaller in magnitude.

### Preconditioned Form for the Two-Dimensional Navier-Stokes Equations

After replacing the density by pressure and temperature using the equation of state ( $\rho = p/RT$ ), the nondimensional form of the unsteady Navier-Stokes equations can be written in generalized nonorthogonal coordinates in a form applicable to both two-dimensional and axisymmetric flow as

$$\frac{\partial Q(\vec{q})}{\partial t} + \frac{\partial (E(\vec{q}) - E_v(\vec{q}))}{\partial \xi} + \frac{\partial (F(\vec{q}) - F_v(\vec{q}))}{\partial \eta} = H(\vec{q}) \quad (5)$$

where

$$\vec{q} = (p, u, v, T)^T,$$

$$Q = \frac{\tau}{J} \left( \frac{p}{RT}, \frac{pu}{RT}, \frac{pv}{RT}, \frac{p}{\gamma R} + \frac{1}{2} \frac{pu^2}{RC_p T} + \frac{1}{2} \frac{pv^2}{RC_p T} \right)^T,$$

$$E = \frac{\tau^\delta}{J} \left( \frac{pU}{RT}, \frac{pU}{RT} + p\xi_x, \frac{pU}{RT} + p\xi_y, \right. \\ \left. pU \left( \frac{1}{R} + \frac{u^2}{2RC_pT} + \frac{v^2}{2RC_pT} \right) \right)^T,$$

$$F = \frac{\tau^\delta}{J} \left( \frac{pV}{RT}, \frac{pV}{RT} + p\eta_x, \frac{pV}{RT} + p\eta_y, \right. \\ \left. pV \left( \frac{1}{R} + \frac{u^2}{2RC_pT} + \frac{v^2}{2RC_pT} \right) \right)^T,$$

$$E_v = \frac{\tau^\delta}{J} (0, \xi_x \tau_{xx} + \xi_y \tau_{xy}, \xi_x \tau_{xy} + \xi_y \tau_{yy}, \\ \xi_x u \tau_{xx} + (\xi_x v + \xi_y u) \tau_{xy} + \xi_y v \tau_{yy} \\ + \frac{\mu}{Pr Re} [(\xi_x^2 + \xi_y^2) T_\xi + (\xi_x \eta_x + \xi_y \eta_y) T_\eta])^T,$$

$$F_v = \frac{\tau^\delta}{J} (0, \eta_x \tau_{xx} + \eta_y \tau_{xy}, \eta_x \tau_{xy} + \eta_y \tau_{yy}, \\ \eta_x u \tau_{xx} + (\eta_x v + \eta_y u) \tau_{xy} + \eta_y v \tau_{yy} \\ + \frac{\mu}{Pr Re} [(\eta_x^2 + \eta_y^2) T_\xi + (\eta_x \xi_x + \eta_y \xi_y) T_\eta])^T,$$

$$H = \frac{\tau^\delta}{J} (0, 0, \frac{\delta}{\tau^\delta} (p - \tau_{\theta\theta}), 0)^T,$$

$$\tau_{xx} = \frac{2}{3} \frac{\mu}{Re} [2(\xi_x u_\xi + \eta_x u_\eta) - (\xi_y v_\xi + \eta_y v_\eta + \delta v/r)],$$

$$\tau_{yy} = \frac{2}{3} \frac{\mu}{Re} [2(\xi_y v_\xi + \eta_y v_\eta) - (\xi_x u_\xi + \eta_x u_\eta + \delta v/r)],$$

$$\tau_{xy} = \frac{\mu}{Re} [(\xi_y u_\xi + \eta_y u_\eta) - (\xi_x v_\xi + \eta_x v_\eta)],$$

$$\tau_{\theta\theta} = \frac{2}{3} \frac{\mu}{Re} [2\frac{v}{r} - (\xi_y v_\xi + \eta_y v_\eta) + (\xi_x u_\xi + \eta_x u_\eta)],$$

$$U = \xi_x u + \xi_y v, \quad V = \eta_x u + \eta_y v$$

In the above,  $\xi$  and  $\eta$  are the spatial coordinates in the generalized system, and  $J$  is the transformation Jacobian. The parameter  $\delta$  is an index indicating the type of flow, two dimensional ( $\delta = 0$ ) or axisymmetric ( $\delta = 1$ ). The parameter  $r$  is the nondimensional distance from the axis of symmetry in the axisymmetric cases. The nondimensional variables are defined as in the one-dimensional case with the addition of  $y = \tilde{y}/L_{ref}$  and  $v = \tilde{v}/u_{ref}$ .

The Navier-Stokes equations given above can also be written as

$$[A_t] \frac{\partial \vec{q}}{\partial t} + [A_\xi] \frac{\partial \vec{q}}{\partial \xi} + [A_\eta] \frac{\partial \vec{q}}{\partial \eta} - [B_\xi] \frac{\partial \vec{q}}{\partial \xi} - [B_\eta] \frac{\partial \vec{q}}{\partial \eta} = H \quad (6)$$

where  $[A_t]$ ,  $[A_\xi]$ ,  $[A_\eta]$ ,  $[B_\xi]$ ,  $[B_\eta]$  are Jacobian matrices defined as

$$[A_t] = \frac{\partial Q}{\partial q}, \quad [A_\xi] = \frac{\partial E}{\partial q}, \quad [A_\eta] = \frac{\partial F}{\partial q},$$

$$[B_\xi] = \frac{\partial E_v}{\partial q}, \quad [B_\eta] = \frac{\partial F_v}{\partial q}$$

In particular, the Jacobian matrix  $[A_t]$  is given by

$$[A_t] = \begin{bmatrix} \frac{1}{RT} & 0 & 0 & -\frac{p}{RT^2} \\ \frac{p}{RT} & \frac{p}{RT} & 0 & -\frac{pu}{RT^2} \\ \frac{p}{RT} & 0 & \frac{p}{RT} & -\frac{pv}{RT^2} \\ \frac{1}{\gamma R} + \frac{1}{2} \frac{u^2 + v^2}{RC_p T} & \frac{pu}{RC_p T} & \frac{pv}{RC_p T} & -\frac{p(u^2 + v^2)}{2C_p RT^2} \end{bmatrix}$$

To enable efficient numerical solution of the system at low Mach numbers, a term  $[A_\tau] \frac{\partial \vec{q}}{\partial \tau}$  is added to the equations where  $\tau$  is a pseudo-time and  $[A_t]$  is a matrix formed by dividing the first column of  $[A_t]$  by  $\gamma M^2$  (equivalent to multiplying the first column of  $[A_t]$  by the nondimensional gas constant

$R$ ). The motivation for this was discussed previously. The equations to be solved numerically become

$$[A_\tau] \frac{\partial \vec{q}}{\partial \tau} + [A_t] \frac{\partial \vec{q}}{\partial t} + [A_\xi] \frac{\partial \vec{q}}{\partial \xi} + [A_\eta] \frac{\partial \vec{q}}{\partial \eta} - [B_\xi] \frac{\partial \vec{q}}{\partial \xi} - [B_\eta] \frac{\partial \vec{q}}{\partial \eta} = H \quad (7)$$

where the matrix  $[A_\tau]$  is given by

$$[A_\tau] = \begin{bmatrix} \frac{1}{T} & 0 & 0 & -\frac{p}{RT^2} \\ \frac{p}{RT} & 0 & 0 & -\frac{pu}{RT^2} \\ \frac{p}{RT} & 0 & \frac{p}{RT} & -\frac{pv}{RT^2} \\ \frac{1}{\gamma} + \frac{1}{2} \frac{u^2 + v^2}{C_p T} & \frac{pu}{RC_p T} & \frac{pv}{RC_p T} & -\frac{p(u^2 + v^2)}{2C_p RT^2} \end{bmatrix}$$

Note that the choice of dependent variables does nothing to alter the conservation law form of the equations.

The equations were discretized and solved numerically using the coupled strongly implicit procedure described by Chen and Pletcher.<sup>8</sup> The scheme utilized central differences, generally (some with deferred corrections<sup>9</sup>), and was first order in time. The equations were linearized by evaluating the Jacobian matrices at the previous pseudo-time step. Time accuracy was maintained by converging the system at each pseudo-time step, at which condition the pseudo-time term vanished. Thus, the converged equations at each physical time step satisfied the discretized Navier-Stokes equations. No smoothing was used for the cases shown here.

For the driven cavity case, no slip boundary conditions were imposed on all boundaries. For the pipe flow cases, no slip conditions were used at the pipe wall. Symmetry conditions were imposed at the centerline. At outflow, the static pressure was specified and all other dependent variables extrapolated from the interior.

In this study it was desired to simulate the startup of pipe flow as realistically as possible. In a typical application, a fixed total pressure is established and maintained at the entrance to the pipe and a valve at the discharge plane is opened. As the flow accelerates from rest, the static pressure of the moving fluid drops. The static pressure and velocities at the pipe inlet and throughout the length of the pipe vary with time until a steady flow is ultimately established. The value of the flow rate finally established will depend upon the difference between the total pressure fixed at the inlet and the fixed discharge pressure and the characteristics of the pipe.

In the numerical simulations, the static pressure at the inlet was extrapolated from the interior and the velocities determined in order to maintain a constant total pressure. In addition, a constant total temperature was specified and the streamwise derivative of the normal component of velocity was taken as zero. That is, the conditions specified at the inlet are

Inlet:

$$p_{i,j} + \frac{P_{i,j}}{RT_{i,j}} u_{i,j}^2 = P_T$$

$$\frac{\partial v_{i,j}}{\partial \xi} = 0$$

$$T_{i,j} + \frac{u_{i,j}^2 + v_{i,j}^2}{2C_p} = T_T$$

where  $P_T$ ,  $T_T$ , are specified and  $p_{i,j}$  is extrapolated from the interior. The boundary conditions were implemented in an implicit fashion. The steady flow profile observed at the

Table 1: Driven Cavity,  $Re = 100$ ,  $19 \times 19$  Grid, Steady Flow, Preconditioned,  $\Delta t = 10^3$ ,  $\Delta t_p = 0.3$

Mach No.	$10^{-5}$	$10^{-3}$	$10^{-1}$	0.2	0.4	0.8	1.0	1.2
No. of Iter.	52	52	52	52	52	52	53	53

Table 2: Driven Cavity,  $Re=100$ ,  $19 \times 19$  Grid, Steady Flow, No conditioning

Mach No.	.01	.1	.1	.1	.2	.2	.4	.4	.4	.8
$\Delta t$	.00025	.02	.025	.03	.05	.1	.15	.2	.25	.3
No. of Iter.	2123	355	302	264	182	138	82	68	97	51

inlet of a two-dimensional channel for such a formulation corresponded well with the results reported by Wang and Longwell.<sup>11</sup>

## RESULTS

### Impulsively Started Driven Cavity

#### Steady State Solution

Prior to undertaking detailed time dependent calculations, the behavior of the preconditioned system was evaluated and compared with unconditioned results over a range of Mach numbers. The computational effort in terms of iterations to achieve steady state is indicated for the preconditioned scheme in Table 1. Notice that the effort is essentially independent of Mach number and that the same pseudo-time step can be used over the entire range of Mach numbers considered. Many of these calculations were repeated on a finer  $39 \times 39$  grid for Mach numbers of 0.4 and lower and the same trend was observed, namely, that the total number of iterations needed to achieve steady state was constant. For the finer grid, 100 iterations were required. The steady state solution was identical for Mach numbers of 0.1 or less.

The computational effort required to obtain the steady flow solution without preconditioning is shown in Table 2. In these calculations it was not possible to use the same time step over a wide range of Mach numbers. Some experimentation was employed with the time step, but it was not easy to predict the optimum time step for a given Mach number. Note that the number of iterations was not reduced to the level achieved with the preconditioning until the Mach number reached 0.8. Convergence was determined for these steady calculations when the residual based on the norm of all variables<sup>10</sup> reached  $10^{-5}$ . The steady flow solution details were virtually independent of Mach number for  $M$  less than about 0.1. The grid stretching was the same for all of the steady cases.

#### Unsteady Solution

For the unsteady driven cavity cases, the fluid was initially at rest and the pressure field was uniform. The unsteady motion started as the cavity lid was impulsively brought to a

Table 3: Driven Cavity,  $Re = 100$ ,  $19 \times 19$  Grid, Unsteady Flow, Preconditioned

Mach No.	$10^{-5}$	$10^{-4}$	$10^{-3}$	$10^{-3}$	$10^{-2}$	$10^{-1}$	0.2
$\Delta t$	0.05	0.05	0.05	0.1	0.05	0.05	0.05
$\Delta t_p$	0.3	0.3	0.3	0.3	0.3	0.3	0.3
Total Iter.	651	652	652	428	652	626	538
Sub-iter.	4	4	4	4	4	4	4

Table 4: Driven Cavity,  $39 \times 39$  Grid, Unsteady Flow, Preconditioned

Mach No.	.001	.001	.1	.2	.2	.4	.001	.1	.2	.4
Re No.	100	100	100	100	100	100	400	400	400	400
$\Delta t$	.025	.025	.025	.025	.025	.025	.05	.05	.05	.1
$\Delta t_p$	.3	.15	.15	.1	.15	.1	.15	.15	.075	.02
Total Iter.	967	980	926	938	881	854	1599	1554	1697	2232
Sub-iter.	4	4	3	3	4	3	4	4	4	10

constant velocity. The computational effort for the unsteady cases were generally independent of Mach number at the low end of the range considered when conditioning was employed. Table 3 indicates the total number of iterations for cases computed on the coarsest grid. The total iterations includes the subiterations required to achieve convergence to  $10^{-5}$  at each time step. The average number of subiterations needed to achieve convergence at each pseudo-time step is also indicated in the table.

On the coarsest grid,  $19 \times 19$ , the total number of iterations for the unsteady cases is seen to reach nearly a constant value of 652 as the Mach number decreases below 0.1. On the  $39 \times 39$  grid, more variation was observed in the total number of iterations as the Mach number was decreased while all other parameters remained fixed, although the variation was less than 10%. A possible explanation for this is as follows. The steady flow cases were computed using a very large physical time step. The result was that the physical time derivative term had no influence on the solution. Only the pseudo-time term influenced the numerics and the preconditioning effectively suppressed the influence of Mach number from that term. Thus, it is not surprising that the solutions become virtually independent of Mach number at the low end, i.e., as the Mach number approaches zero. For true transient calculations, however, the physical time term remains, and the time step needs to be sufficiently small to achieve time accuracy. The physical time term behaves like a source term during the pseudo-time iterations, and the size of the source term varies with Mach number. Thus, there may be no reason to expect the total iteration count to be rigidly independent of Mach number for time accurate calculations. This aspect of time-accurate preconditioned methods has not received much attention until now. Only a few unsteady cavity cases were computed without preconditioning. The computational effort required for the unconditioned scheme is summarized in Table 5.

Note that the number of iterations increases significantly as the Mach number decreases below 0.2. Note also that subiterations were required at each time step even without the use of pseudo-time. The iterations were required to remove the linearization errors and converge the pressure

Table 5: Driven Cavity,  $Re = 100$ , Unsteady Flow, No Conditioning

Mach No.	0.01	0.1	0.2	0.2	0.4	0.6
Grid	39×39	39×39	19×19	39×39	19×19	19×19
$\Delta t$	0.001	0.01	0.05	0.025	0.1	0.05
Total Iter.	5288*	1883	905	1167	423	472
Sub-iter.	4	4	5	4	4	3

\*This case was only computed to  $t=1.34$  whereas steady state is achieved at approximately 6 time units.

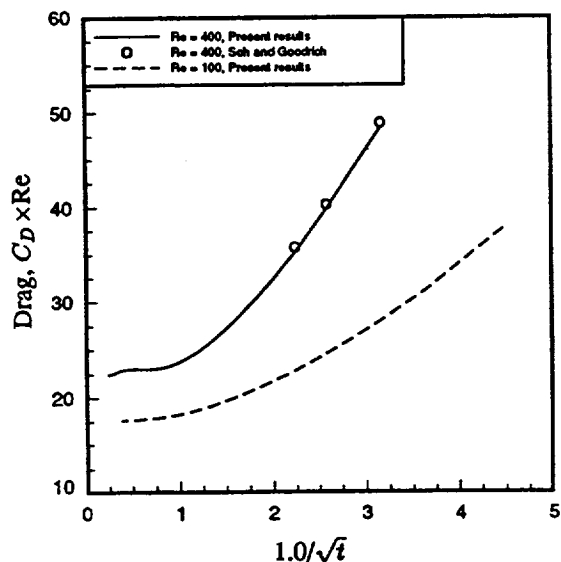


Figure 1: Behavior of drag force at early times, impulsively started cavity.

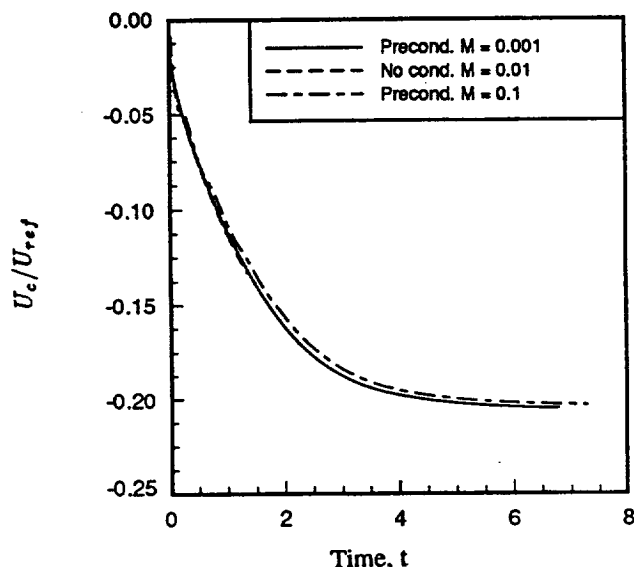


Figure 2: Time history of predicted  $u$  component of velocity at cavity center,  $Re=100$ , impulsively started cavity.

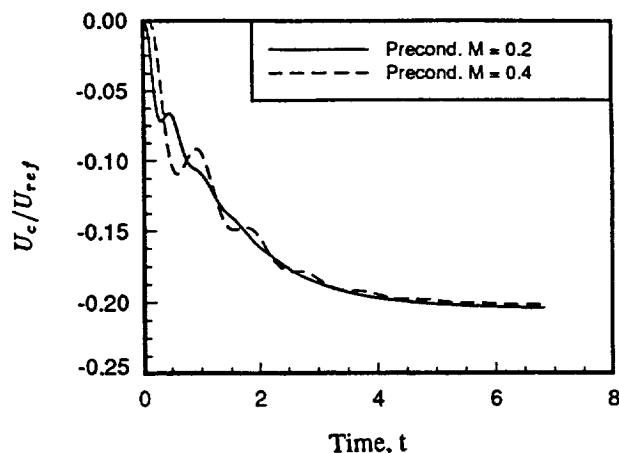


Figure 3: Time history of predicted  $u$  component of velocity at cavity center,  $Re=100$ , impulsively started cavity.

field. The number of subiterations can be seen to decrease as the Mach number increases. At Mach numbers of 0.01 and below, the transient results were in good agreement with those obtained by others<sup>12</sup> using purely incompressible formulations. Figure 1 compares the variation of the drag coefficient with time obtained with the present preconditioned compressible scheme with the computational results obtained by Soh and Goodrich.<sup>12</sup> The nondimensional time,  $t$ , in the figures for the cavity flow calculations is defined as  $t = \tilde{t} / (L / U_{ref})$ .

Many aspects of steady driven cavity flow have been reported in the literature, particularly velocity profiles. Some aspects of unsteady incompressible driven cavity flow particularly the time history of the flow patterns have been reported by Soh and Goodrich<sup>12</sup>. These will not be repeated here.

The time history of the computed  $u$  component of velocity at the center of the cavity is given in Fig. 2 for  $M=0.001$ , 0.01 and 0.1. The computations were carried out on a  $39 \times 39$  grid. No conditioning was used for the results reported for  $M=0.01$ . At first glance it is easy to conclude that the time history is essentially the same for these three Mach numbers. Closer inspection reveals a slight wiggle in the velocity for  $M=0.1$  at small nondimensional times. This was easy to ignore at first in this study, but it is now believed that this behavior is a real part of impulsively started compressible driven cavity flows. The oscillation in the velocity at the center becomes more pronounced as the Mach number increases, and as indicated in Fig. 3, where results for  $M=0.2$  and 0.4 are shown, it cannot be ignored or considered an aberration.

A very similar behavior can be observed in the solutions obtained without conditioning. That is, the oscillatory behavior appears not to be a product of the preconditioned formulation. This is indicated in Fig. 4 where both preconditioned results and results obtained without conditioning are shown for  $Re=100$  on the  $39 \times 39$  grid. The two results are nearly identical. Also shown in Fig. 4 are preconditioned results obtained on a  $79 \times 79$  grid. The oscillatory results are more sharply resolved on the finer grid, but the qualitative picture remains the same.

A possible explanation for this behavior is as follows. The impulsive start of the cavity lid creates a singularity in the flow field. That is, an absolutely impulsive start is not physically



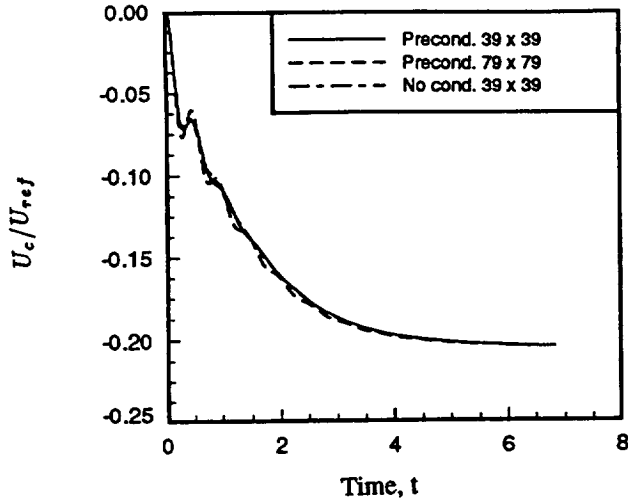


Figure 4: Effect of grid refinement on time history of  $u$  component of velocity at cavity center,  $Re=100$ , impulsively started cavity.

possible. Any real start of the motion must occur over a finite interval of time. In their incompressible work, Soh and Goodrich pointed out a square root singularity in the drag on the moving lid. The fact that the drag curve in Fig. 1 is linear at small times tends to verify this singular behavior. To resolve the flow accurately at very small times, finer and finer spatial resolution is required. For purely incompressible flow, the effects of the singularity are transmitted only by convection and diffusion. The initial pressure has no influence on the solution. Acoustic signals are transmitted instantaneously so any influence that the abrupt start has on the pressure field is mitigated by the rapid propagation of signals.

The magnitude of the reference Mach number in this problem is precisely the nondimensional time required for an acoustic wave to move the length of the cavity if propagating at the sonic speed corresponding to the reference temperature. For calculations at very low Mach numbers, an acoustic wave could make several traverses across the cavity during the first time step. This leads to the results seen in Fig. 2 which is exactly the behavior of solutions to the incompressible equations. At very low Mach numbers, the physical time term (source term for solution advancement in pseudo-time) is very small, and the effect of pressure history is correspondingly small. For the calculations at  $M=0.1$ , the time required for acoustic waves to traverse the cavity is about 0.1 nondimensional time units. This time interval is now larger than the computational time step required to maintain temporal accuracy and a slight oscillation can be observed in Fig. 2. The oscillations can be seen more clearly in Fig. 3. The period of the initial oscillations observed in Fig. 2 is approximately 0.4 for the  $M=0.2$  results and 0.8 for the  $M=0.4$  results. The periods are approximately the time required for acoustic waves to propagate across the cavity and back. The oscillations are seen to damp out as the solution tends toward steady state. The pressure at the center of the cavity is observed to possess a similar oscillatory pattern as can be seen in Fig. 5. The  $p_{ref}$  in Fig. 5 is the pressure value at the center of the bottom plate of the cavity.

The oscillatory pattern is seen to sharpen somewhat when

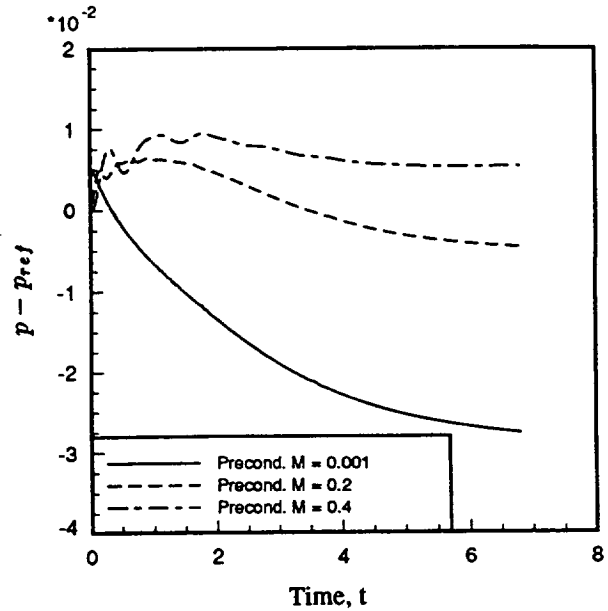


Figure 5: Time history of predicted pressure at cavity center,  $Re=100$ , impulsively started cavity.

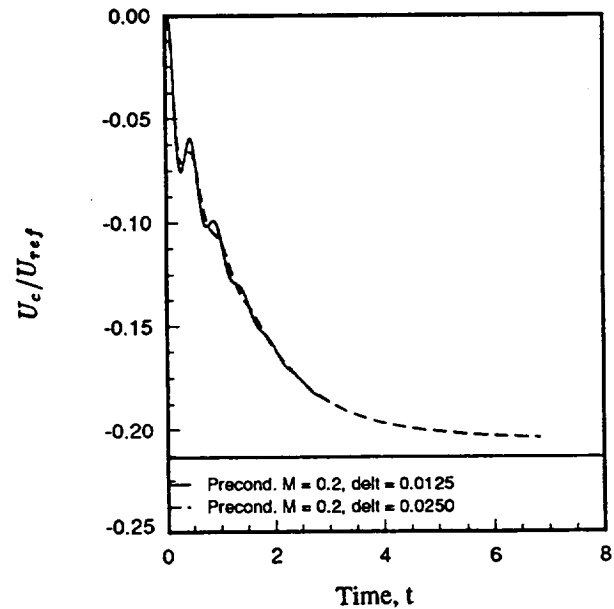


Figure 6: Effect of time step on the time history of  $u$  component of velocity at cavity center,  $Re=100$ , impulsively started cavity.

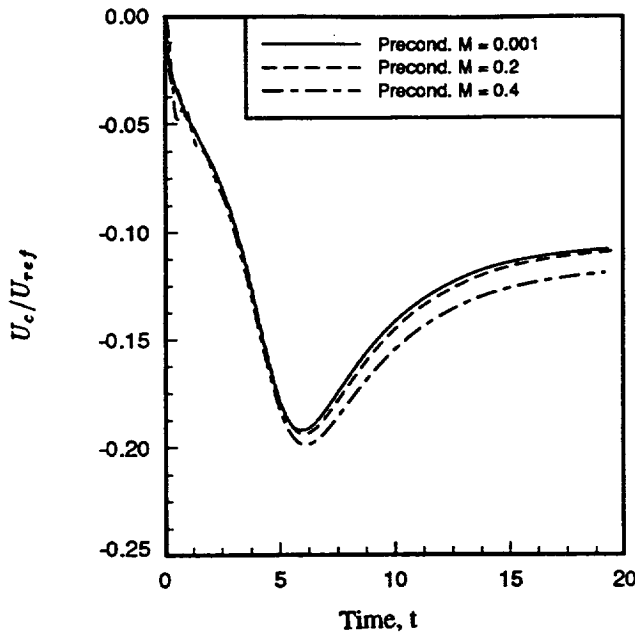


Figure 7: Time history of  $u$  component of velocity at cavity center,  $Re=400$ , impulsively started cavity.

a smaller physical time step is employed as can be seen in Fig. 6. This is reasonable since the phenomenon is believed to originate with the impulse associated with the start of the lid. The smallest time step that will permit the viscous region to reach the first grid point from the wall (for the  $39 \times 39$  grid) in an analogy with the impulsively started flat plate is about 0.0125 corresponding to the solid line results in Fig. 6. The trends observed for a Reynolds number of 400 are somewhat similar in that oscillatory behavior was observed for Mach numbers of about 0.2 or larger. The flow at  $Re=400$  is actually quite different and the time history is quite interesting<sup>12</sup>. For example, the history of the velocity at the center is not monotonic and the nondimensional time required for the flow to reach a steady state is 2-3 times as long as for the flow at  $Re=100$ . Figure 7 shows the history of the  $x$ -component velocity for calculations at Mach numbers of 0.001, 0.2, and 0.4. Oscillations are detectable in the  $M=0.2$  and 0.4 results. Again, the initial periods of the oscillations are about 0.4 and 0.8, respectively, although this is not evident from the plots.

### Startup of Pipe Flow

A goal of the present study has been to evaluate the time accuracy of preconditioned schemes with a view toward determining the merits of using a single scheme for simulating both incompressible and compressible phenomena. The startup of flow in a pipe is a real transient phenomena that can be observed in the laboratory with greater ease than the impulsively started cavity considered above. Pipe flow is a pressure driven flow whereas the cavity is a shear driven flow and it was speculated that compressibility effects might play a more dominant role in the physics of transient pressure driven flows.

Incompressible starting pipe flow has been studied computationally through solutions to the Navier-Stokes equations

by Anderson and Kristoffersen<sup>13</sup> and through solutions to the boundary-layer equations by Ramin and Pletcher.<sup>14</sup> For an infinitely long pipe (no entrance effects) and incompressible flow, the governing equations for the startup problem become linear and a solution in the form of Bessel functions was proposed by Szymanski.<sup>15</sup> For pipes of finite length, a flow development region exists and the flow is governed by the nonlinear Navier-Stokes equations. Except for small Reynolds numbers, the boundary-layer approximation can provide a model that provides reasonably accurate solutions over most of the development length under incompressible assumptions. The full Navier-Stokes equations were used in the present study.

In the transient pipe flow problems considered here, the total pressure was considered to be fixed at the pipe inlet. The static pressure at the pipe discharge was also fixed and this pressure difference [ $H = P_{total} \text{ (at inlet)} - P_{static} \text{ (at discharge)}$ ] became part of the problem specification. The appropriate characteristic velocity for this transient flow is not obvious. The final steady flow velocity (or mass flow rate) is not known *a priori*. One physically relevant characteristic velocity is given by  $U_p = (H/\rho)^{1/2}$ , the maximum velocity that could be achieved from an application of Bernoulli's equation on a lumped (stream tube) basis to this flow. A second one is the average velocity that would exist in incompressible laminar fully developed flow consuming the pressure drop  $H$ ,  $V_{inf} = \frac{HD^2}{32\mu L}$ .

Otis<sup>16</sup>, working with incompressible flow assumptions, proposed the use of the nondimensional parameter  $E = \frac{1}{2048} \left( \frac{Re_p D}{L} \right)^2$ , where  $Re_p$  is the Reynolds number based on diameter and  $U_p$ , (Otis and others used  $M$  for this parameter but  $M$  is not appropriate here) to characterize this startup flow. Note that  $E=0$  corresponds to flow in an infinitely long pipe. The parameter  $E$  can be thought of as the ratio of the time scales for cross stream diffusion and streamwise convection. The value of  $E$  will also determine how closely the steady state flow rate will approach the flow that would be predicted by considering  $H$  to be the static pressure drop for fully developed laminar flow. The larger the value of  $E$ , the smaller the flowrate compared to the flow that would result if the  $H$  were consumed by pressure drop in fully developed laminar flow. In other words, the larger the value of  $E$ , the greater the entrance effect and its corresponding momentum pressure drop. Nearly all of the previous literature on this subject dealt with incompressible flow. All computations were made using air as the working fluid, isothermal wall conditions with the Prandtl number set equal to 1.0. The Mach number reported for the pipe results was based on the  $V_{inf}$  reference velocity defined above and the sonic velocity based on the inflow stagnation temperature.

It was of interest first to determine if the present compressible formulation could duplicate all the expected physics for a purely incompressible flow. To this end, computations were made for the startup problem using a Mach number of  $1.386 \times 10^{-3}$ . Calculations were made for  $E=0.084$ , 0.108, and 0.5. Two grids were employed for the  $E=0.108$  case. To simulate incompressible flow calculations correctly, at all time steps the mass flow rate should be everywhere the same in the pipe since the density of an incompressible fluid would not change with time. This was achieved to within less than 0.5%. In terms of the nondimensional equations, the small value of Mach number is effectively suppressing the physical time term in the continuity equation.

Figure 8 shows the time history of the mass flow rate for

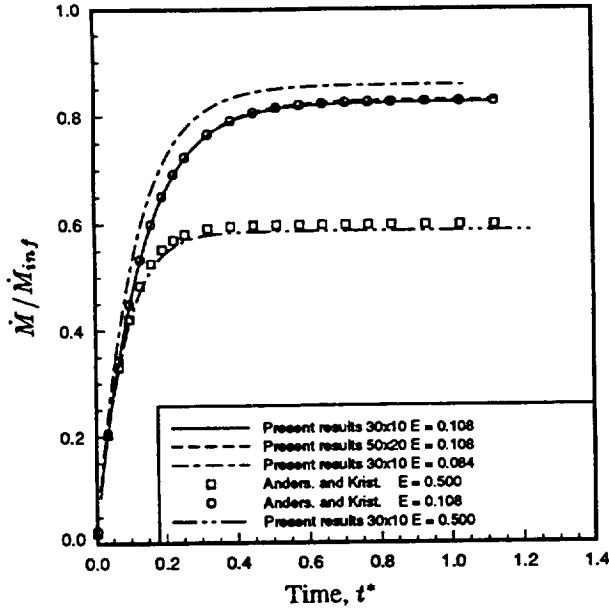


Figure 8: Time history of predicted ( $M=0.001386$ ) pipe discharge rate for several values of  $E$ .

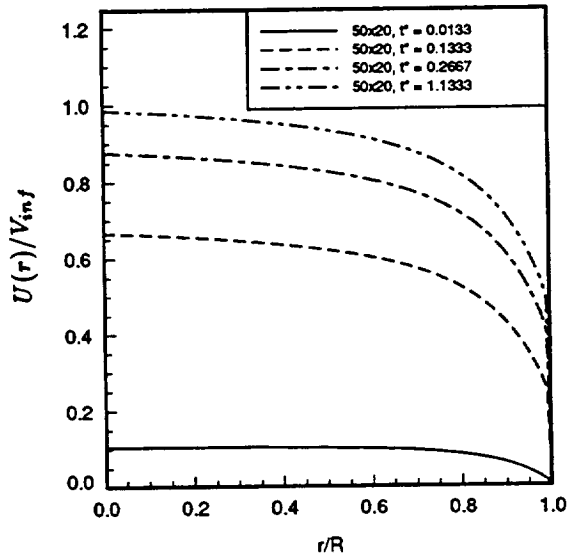


Figure 9: Predicted pipe inlet velocity distributions at various times,  $M=0.001386$ ,  $E=0.108$ .

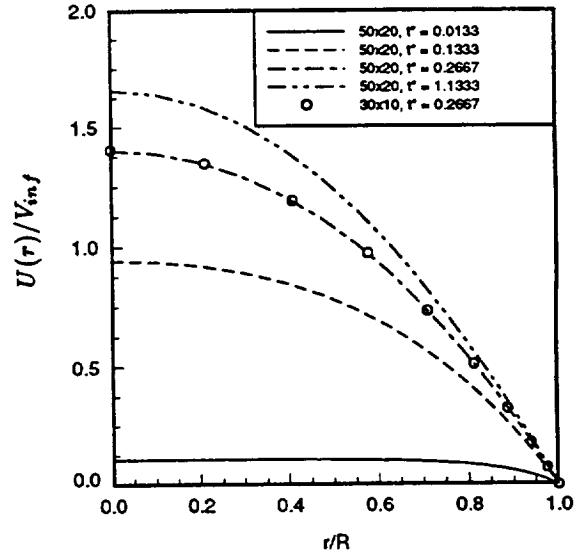


Figure 10: Predicted pipe discharge velocity distributions at various times,  $M=0.001386$ ,  $E=0.108$ .

the  $M=1.386 \times 10^{-3}$  cases computed. The nondimensional time,  $t^*$ , in the figures for the pipe flow calculations is defined as  $t^* = \bar{t}/(\frac{R^2}{\nu})$ . The flowrate in the figure has been nondimensionalized with the flowrate that would be achieved for a fully developed incompressible laminar flow consuming the same pressure drop in the same tube, i.e., based on an average velocity of  $V_{inf}$  defined above. The present results are seen to be in good agreement with the numerical results of Anderson and Kristoffersen<sup>13</sup>, especially for  $E=0.108$ . Grid refinement for that case made little difference in the results as can be seen in Fig. 8. The flow at  $E=0.108$  reaches the fully developed state with the centerline velocity equal to twice the average velocity. For the  $E=0.5$  case, the centerline velocity was 3% short of the fully developed value. Velocity profiles at inlet and at the discharge are shown in Figs. 9 and 10. It is of interest to note that the inlet velocity distribution is not uniform under the present method of fixing the total pressure at inlet.

The transient behavior of flow was strikingly different for the higher Mach number cases computed. At early times, the fluid in the pipe "decompressed" allowing flow to discharge from the pipe while the inlet flow was zero. This can be seen in Fig. 11. At the earliest time shown, one third to one half of the fluid is at rest as fluid is forced out the discharge at flow rates sometimes higher than the steady state values. The variation of the discharge rate with time for three cases,  $M=0.1386$ ,  $M=0.2772$  and  $M=0.3224$  are shown in Fig. 12. This is in contrast to the results of the lowest Mach number case (effectively incompressible) shown in Fig. 8. Even though the steady flow behavior of all of these cases may be close to that attributed to incompressible flow, the transient behavior is greatly different. A design based on incompressible results shown in Fig. 8 may not work for flows at speeds as low as approximately Mach 0.1.

The time history of the centerline pressure is shown in Fig. 13 for the two highest Mach number cases. The pressure remains at nearly the total pressure for the majority of the pipe for the earliest time shown. In contrast, for an incompressible

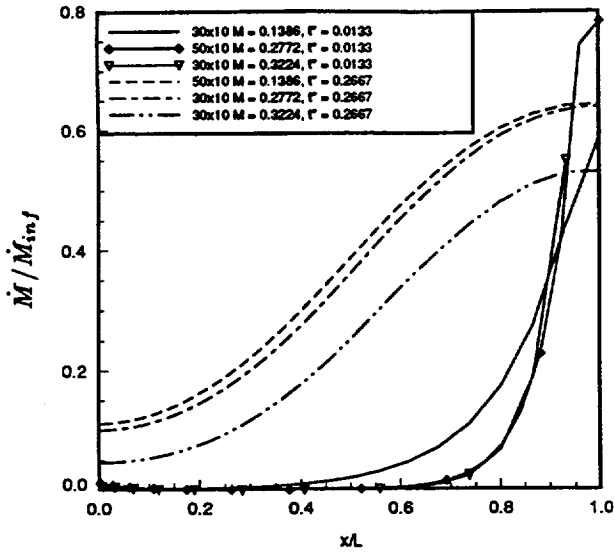


Figure 11: Predicted distribution of flow rate along pipe at early times,  $E=0.108$ .

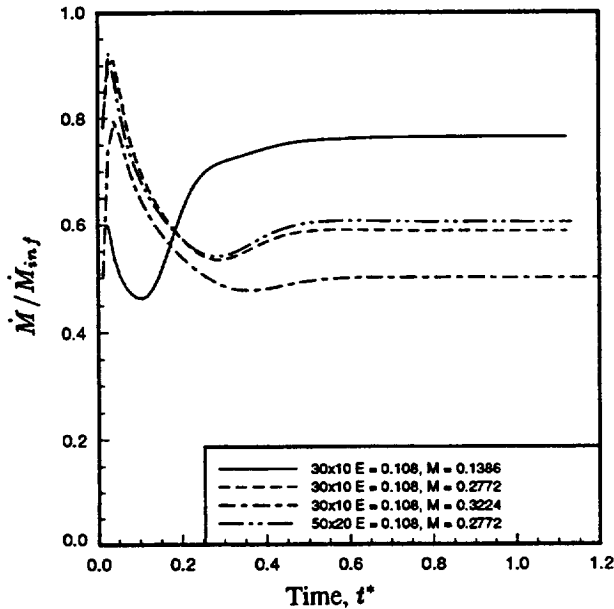


Figure 12: Predicted time history of pipe discharge at three values of Mach number,  $E=0.108$ .

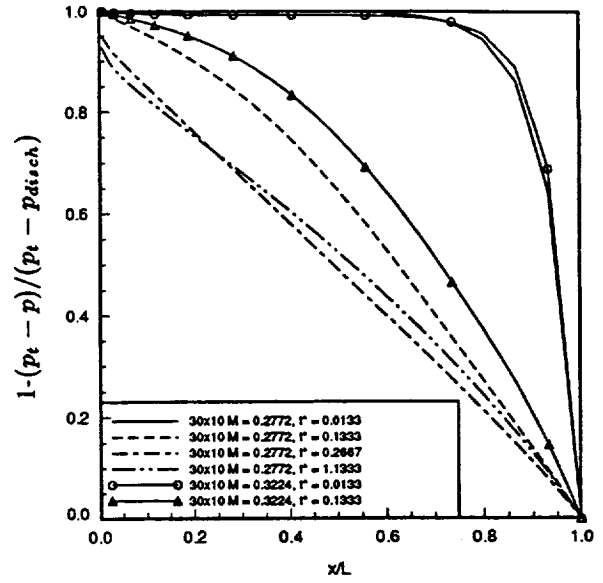


Figure 13: Predicted distribution of centerline pressure along pipe at early times,  $E=0.108$ .

case (not shown in Fig. 13) the earliest pressure would be more like the large time curves shown in Fig. 13. For the pipe flow cases, the nondimensional time required for an acoustic wave, moving at the sonic speed corresponding to the inlet total temperature, to travel the length of the pipe is given by  $M/(16E)$ .

The computing effort required for the pipe cases varied noticeably over the Mach number range. This is in contrast to the driven cavity case where the physics did not change much as the Mach number varied. In the pipe flow case, the flow was driven by pressure differences. At the lowest Mach number considered, essentially no motion could occur until the pressure field was established in line with the boundary conditions and flow occurred simultaneously throughout the entire computational domain. On the other hand, essentially no action occurred in a large portion of the pipe at early times for the higher Mach number cases. Constant time steps of  $t^*=0.0133$  were used for all results shown. Approximately 85 time steps were needed to achieve the steady state conditions. Most of the calculations were carried out on a  $30 \times 10$  grid but two calculations were made on  $50 \times 20$  grids for evaluation of the effects of grid refinement. The convergence criteria for each time step was set at  $10^{-6}$  for the pipe flow cases. For steady pipe flow calculations, starting with the fluid at rest, 718 iterations were required for the  $M=0.001386$  case and 933 for the  $M=0.2772$  case both on a  $50 \times 20$  grid. For the finest grid unsteady flow calculations, however, an average of 310 iterations was required for convergence at each time step for the  $M=0.001386$  case whereas only an average of 61 iterations was required per time step for the  $M=0.2772$  case. This difference was not anticipated in light of the experience reported for the driven cavity transient calculations. Whether this is reasonable in light of the the complexity of the physics is presently under study.

## CONCLUSION

Generally, the coupled, preconditioned compressible formulation was observed to perform well over a range of Mach numbers for two transient test cases. For the driven cavity flow, the computational effort was nearly independent of Mach number especially at low values although this was more precisely true for the steady cavity calculations than for the transient ones. The impulsive start of the cavity lid was observed to promote an oscillatory behavior in the velocities and pressure that was not observed at the lowest Mach numbers. The preconditioned results, including the oscillatory velocities, were in good agreement with results obtained without preconditioning.

The calculations of the startup of pipe flow obtained for a very small Mach number,  $M=0.001386$ , were in agreement with results obtained by Anderson and Kristoffersen<sup>13</sup> who solved the incompressible equations. For the higher Mach numbers considered, the transient behavior was entirely different in that the flow started by decompression while the inlet mass flow remained essentially zero. That this should be true can be reasoned taking into account the time required for acoustic waves to penetrate from the discharge plane to the inlet and the compressibility of the fluid. Conservation of mass can be maintained without inflow as the density changes with time. The computational effort required to solve the lowest Mach number case for the pipe startup was substantially greater than that required for the higher Mach number cases. Such a dependency has not been observed for previous steady flow calculations. This issue is presently under study.

## ACKNOWLEDGEMENTS

This research was partially supported by the Institute for Computational Mechanics in Propulsion at NASA Lewis Research Center under NASA Cooperative Agreement NCC3-233.

## REFERENCES

1. Turkel, E., "Preconditioned Methods for Solving the Incompressible and Low Speed Compressible Equations," *Journal of Computational Physics*, Vol. 72, 1987, pp. 277-298.
2. Turkel, E., "Review of Preconditioning Methods for Fluid Dynamics," ICASE Report No. 92-47, Institute for Computer Applications in Science and Engineering, NASA Langley Research Center, Hampton Virginia, 1992.
3. Feng, J. and Merkle, C. L., "Evaluation of Preconditioning Methods for Time-Marching Systems," AIAA Paper 90-0016, 1990.
4. Peyret, R. and Viviand, H., "Pseudo-Unsteady Methods for Inviscid or Viscous Flow Computations," *Recent Advances in the Aerospace Sciences*, C. Casci, Ed., Plenum Press, N.Y., 1985, pp. 312-343.
5. Choi, D. and Merkle, C. L., "Time-Derivative Preconditioning for Viscous Flows," AIAA Paper 91-1652, 1991.
6. Chorin, A. J., "A Numerical Method for Solving Incompressible Viscous Flow Problems," *Journal of Computational Physics*, Vol. 2, 1967, pp. 12-26.
7. Shuen, J.-S., Chen, K.-H., and Choi, Y., "A Time-Accurate Algorithm for Chemical Non-Equilibrium Viscous Flows at All Speeds," AIAA Paper 92-3639, 1992.
8. Chen, K.-H. and Pletcher, R. H., "Primitive Variable, Strongly Implicit Calculation Procedure for Viscous Flows at All Speeds," AIAA Journal Vol. 29, No. 8, August 1991, pp. 1241-1249.
9. Jorgenson, P. C. E., "An Implicit Numerical Scheme for the Simulation of Internal Viscous Flows on Unstructured Grids," Ph.D. Dissertation, Iowa State University, 1992.
10. Withington, J. P., Shuen, J. S., and Yang, V., "A Time Accurate Implicit Method for Chemically Reacting Flows at All Mach Numbers," AIAA Paper 91-0581, 1991.
11. Wang, Y. L. and Longwell, P. A., "Laminar Flow in the Inlet Section of Parallel Plates," *AIChE Journal*, Vol. 10, 1964, pp. 323-329.
12. Soh, W. Y. and Goodrich, J. W., "Unsteady Solution of Incompressible Navier-Stokes Equations," *Journal of Computational Physics*, Vol. 79, 1988, pp. 113-134.
13. Anderson, H. I. and Kristoffersen, R., "Start-Up of Laminar Pipe Flow," *Proc. AIAA/ASME/SIAM/APS 1st National Fluid Dynamics Congress*, 1988, pp. 1356-1363.
14. Ramin, T. H. and Pletcher, R. H., "Developments on an Unsteady Boundary-Layer Analysis: Internal and External Flows," *Numerical Heat Transfer, Part B*, 1993 (in press).
15. Szymanski, F., "Quelques Solutions Exactes des Equations de l'Hydrodynamique du Fluide Visqueux dans le Case d'un Tube Cylindrique," *Journal des Mathematiques Pure et Appliquees*, Vol. 11, 1932, pp. 67-107.
16. Otis, D. R., "Laminar Start-Up Flow in a Pipe," *ASME Journal of Applied Mechanics*, Vol. 52, 1985, pp. 706-711.

REPORT DOCUMENTATION PAGE			Form Approved OMB No. 0704-0188	
Public reporting burden for this collection of information is estimated to average 1 hour per response, including the time for reviewing instructions, searching existing data sources, gathering and maintaining the data needed, and completing and reviewing the collection of information. Send comments regarding this burden estimate or any other aspect of this collection of information, including suggestions for reducing this burden, to Washington Headquarters Services, Directorate for Information Operations and Reports, 1215 Jefferson Davis Highway, Suite 1204, Arlington, VA 22202-4302, and to the Office of Management and Budget, Paperwork Reduction Project (0704-0188), Washington, DC 20503.				
1. AGENCY USE ONLY (Leave blank)	2. REPORT DATE July 1993	3. REPORT TYPE AND DATES COVERED Technical Memorandum		
4. TITLE AND SUBTITLE On Solving the Compressible Navier-Stokes Equations for Unsteady Flows at Very Low Mach Numbers		5. FUNDING NUMBERS  WU-505-90-5K		
6. AUTHOR(S)  R.H. Pletcher and K.-H. Chen				
7. PERFORMING ORGANIZATION NAME(S) AND ADDRESS(ES)  National Aeronautics and Space Administration Lewis Research Center Cleveland, Ohio 44135-3191		8. PERFORMING ORGANIZATION REPORT NUMBER  E-8193		
9. SPONSORING/MONITORING AGENCY NAME(S) AND ADDRESS(ES)  National Aeronautics and Space Administration Washington, D.C. 20546-0001		10. SPONSORING/MONITORING AGENCY REPORT NUMBER  NASA TM-106380 ICOMP-93-42 AIAA-93-3368		
11. SUPPLEMENTARY NOTES Prepared for the 24th Fluid Dynamics Conference, sponsored by the American Institute of Aeronautics and Astronautics, Orlando, Florida, July 6-9, 1993. R.H. Pletcher, Institute for Computational Mechanics in Propulsion, NASA Lewis Research Center and Iowa State University, Ames, Iowa 50010; K.-H. Chen, Ohio Aerospace Institute, 22800 Cedar Point Road, Brook Park, Ohio 44142 and University of Toledo, Toledo, Ohio 43606, (work funded under NASA Cooperative Agreement NCC3-233). ICOMP Program Director, Louis A. Povinelli, (216) 433-5818.				
12a. DISTRIBUTION/AVAILABILITY STATEMENT  Unclassified - Unlimited Subject Categories 34 and 64			12b. DISTRIBUTION CODE	
13. ABSTRACT (Maximum 200 words)  The properties of a preconditioned, coupled, strongly implicit finite-difference scheme for solving the compressible Navier-Stokes equations in primitive variables are investigated for two unsteady flows at low speeds, namely the impulsively started driven cavity and the startup of pipe flow. For the shear-driven cavity flow, the computational effort was observed to be nearly independent of Mach number, especially at the low end of the range considered. This Mach number independence was also observed for steady pipe flow calculations; however, rather different conclusions were drawn for the unsteady calculations. In the pressure-driven pipe startup problem, the compressibility of the fluid began to significantly influence the physics of the flow development at quite low Mach numbers. The present scheme was observed to produce the expected characteristics of completely incompressible flow when the Mach number was set at very low values. Good agreement with incompressible results available in the literature was observed.				
14. SUBJECT TERMS  Preconditioning; Unsteady flow; Compressible flow			15. NUMBER OF PAGES 12	
			16. PRICE CODE A03	
17. SECURITY CLASSIFICATION OF REPORT Unclassified	18. SECURITY CLASSIFICATION OF THIS PAGE Unclassified	19. SECURITY CLASSIFICATION OF ABSTRACT Unclassified	20. LIMITATION OF ABSTRACT	



National Aeronautics and  
Space Administration

**Lewis Research Center**

Cleveland, OH 44135-3191  
ICOMP OAI

Official Business

Penalty for Private Use \$300